1042 *Biochemistry* **2010,** *49,* 1042–1052
DOI: 10.1021/bi901813e

BIOCHEMISTRY
including biophysical chemistry & molecular biology
Article

Role of Prolyl *cis*/*trans* Isomers in Cyclophilin-Assisted *Pseudomonas syringae* AvrRpt2 Protease Activation[†]

Tobias Aumüller, Günther Jahreis, Gunter Fischer,* and Cordelia Schiene-Fischer*

Max-Planck Research Unit for Enzymology of Protein Folding, Weinbergweg 22, D-06120 Halle/Saale, Germany

Received October 23, 2009; Revised Manuscript Received December 17, 2009

ABSTRACT: In a process contributing to the innate immunity of higher plants, *Arabidopsis thaliana* cyclophilin ROC1 induces the self-cleavage of *Pseudomonas syringae* putative cysteine protease AvrRpt2, triggering limited cleavage of *A. thaliana* RIN4, a negative regulator of plant immunity. We report an increase in AvrRpt2 activity in hydrolysis of decapeptide substrates at -GG- sites of more than 5 orders of magnitude, in the presence of cyclophilin-like peptidyl prolyl *cis*/*trans* isomerases including ROC1 or hCyp18. Both full-length AvrRpt2 and its 21 kDa self-cleavage product ($AvrRpt2^{72-255}$) were found to be equally active under these conditions. In contrast to classical isomer-specific proteolysis, inertness toward cleavage of a *cis*/*trans* prolyl bond isomer at the substrate P4 subsite is not the cause of cyclophilin-mediated activation of the proteolytic reaction. Monitoring single- and double-jump kinetics of proteolytic reactions in the presence of the PPIase inhibitor cyclosporin A revealed that the *cis*/*trans* ratio of potentially relevant prolyl bonds of $AvrRpt2^{72-255}$ remained the same in the functionally inactive state of $AvrRpt2^{72-255}$ and the productive $AvrRpt2^{72-255}$−cyclophilin−substrate complex.

When delivered into the *Arabidopsis* host cell via the type III secretion system, the phytopathogenic *Pseudomonas syringae* 28 kDa AvrRpt2 protein undergoes specific proteolytic self-cleavage between residues Gly^{71} and Gly^{72}. Of the two cleavage products, a 9 kDa peptide ($AvrRpt2^{1-71}$) and the carboxy-terminal 21 kDa protein ($AvrRpt2^{72-255}$), the larger fragment was shown to induce the RPS2-dependent plant defense response causing the proteolytic removal of the host protein RIN4 (*1*−*3*). This process takes part in the innate immunity of higher plants (*4*). Pioneering studies by Staskawicz and his co-workers demonstrated that the *Arabidopsis* folding helper protein ROC1 serves to trigger both self-cleavage of AvrRpt2 and limited degradation of RIN4 at two AvrRpt2-related cleavage sites. The reaction probably utilizes the predicted cysteine protease catalytic triad of AvrRpt2 (C122, H208, and D226) typical of a staphopain-like enzyme (*5*, *6*). The finding that only AvrRpt2 and not $AvrRpt2^{72-255}$ could physically interact with GST-fused ROC1[1] apparently indicated a transient folding assistance by ROC1 for AvrRpt2 (*5*). ROC1 is a constitutively expressed prototypic peptidyl prolyl *cis*/*trans* isomerase (PPIase) of the plant cytosol belonging to the large subfamily (totaling 29 members) of *Arabidopsis* cyclophilins (*7*). Consequently, the cyclophilin inhibitor cyclosporin A (CsA) abolishes ROC1-mediated self-processing of AvrRpt2 (*5*). Recently, other PPIase-activated proteolytic reactions have been suggested to play an important role in human infectious diseases, though detailed molecular data are lacking (*8*, *9*). The PPIase domains of cyclophilins share the common functional properties by providing proline-directed binding affinity to unfolded, partially folded, and native states of protein chains and by enhancing *cis* to *trans* and *trans* to *cis* isomerization rates by up to 10^6-fold compared to the rate of uncatalyzed conformational interconversion (*10*). In fact, prolyl isomer-specific proteolysis is based on a nearly completely unreactive *cis* prolyl isomer of a substrate as exemplified by tryptic and chymotryptic cleavage of oligopeptides with a proline residue positioned in the P2 subsite [nomenclature according to Schechter and Berger (*11*)] (*12*, *13*). In the presence of optimal concentrations of a highly efficient protease, the uncatalyzed *cis* to *trans* isomerization of a prolyl bond can become rate-limiting. The substrate remains fully cleavable but at the cost of biphasic reaction kinetics. Upon catalysis by a PPIase, the biphasic character gradually changes with the concentration of the catalyst to produce monophasic behavior at high PPIase activities. AvrRpt2 contains 13 proline residues, one of which is located at position P4 of its Gly^{71}-Gly^{72} cleavage site. A proline residue is also present at the P4 site of RIN4. Notably, the P4 proline is functionally important as an AvrRpt2 P68A mutant displays diminished self-processing (*14*). Whether the prolyl isomerization of the Val^{67}-Pro^{68} moiety may constitute a critical factor in ROC1-assisted proteolysis reactions has not been previously tested.

The current molecular model of ROC1-mediated self-cleavage of AvrRpt2 postulates that Gly-Pro-Xaa-Leu sequence stretches

[†]Supported by the Deutsche Forschungsgemeinschaft (Grant SFB 610 to G.F. and Grant GRK 1026 to C.S.-F.) and the Fonds der Chemischen Industrie (to T.A.).

*To whom correspondence should be addressed. G.F.: Weinbergweg 22, D-06120 Halle/Saale, Germany; e-mail, fischer@enzyme-halle.mpg.de; phone, +49 345 5522800; fax, +49 345 5511972. C.S.-F.: Weinbergweg 22, D-06120 Halle/Saale, Germany; e-mail, schiene@enzyme-halle.mpg.de; phone, +49 345 5522809; fax, +49 345 5511972.

[1]Abbreviations: Abz, 2-aminobenzoyl; AEBSF, 4-(2-aminoethyl)-benzenesulfonyl fluoride; CsA, cyclosporin A; hCyp18, human cyclophilin 18; DTT, 1,4-dithiothreitol; E-64, *trans*-epoxysuccinyl-L-leucylamido-(4-guanidino)butane; ESI-MS, electrospray mass spectrometry; GST, glutathione *S*-transferase; ITC, isothermal titration calorimetry; MALDI-TOF, matrix-assisted laser desorption ionization time-of-flight; PPIase, peptidyl prolyl *cis*/*trans* isomerase; prolyl isomerization, *cis*/*trans* isomerization of the Xaa−Pro peptide bond; prolyl bond, peptide bond preceding a proline residue; RPS2, *Arabidopsis* resistance gene locus; ROC1, Rotamase cyclophilin 1; RIN4, RPM1 interacting protein 4; TCEP, tris(2-carboxyethyl)phosphine; TFA, trifluoroacetic acid; TFE, trifluoroethanol; TIS, triisopropylsilane; y, 3-nitrotyrosine.

 Published on Web 01/05/2010

containing the 12 remaining proline residues adopt a *trans* isomeric state representing the protease-inactive state of AvrRpt2. Upon formation of the AvrRpt2−ROC1 complex, readjustment of Gly-Pro backbone stretches in the native fold of AvrRpt2 is proposed to favor the formation of *cis* prolyl bonds. The resulting conformational state of AvrRpt2 might constitute the active protease (*6*). This hypothetical mechanism agrees with other investigations showing that a higher *cis*/*trans* ratio of proline-containing ligands can be found in Michaelis or encounter cyclophilin−substrate complexes compared to the ratio of isomers in the unbound ligand (*16*−*20*). It is also evident that the conformation of a single peptide bond can separate protein states of distinct biological activity in vitro and in vivo (*21*−*27*). Notably, actual catalysis of prolyl isomerization is not stringently required in the proposed molecular model of AvrRpt2 activation. Nevertheless, the enzyme specificity of the assisting PPIase appears to play a role as *Saccharomyces cerevisiae* CPR1 (*5*) and rabbit reticulocyte lysate cyclophilins but not *Escherichia coli* cyclophilins (*15*) could activate the self-cleavage reaction (*5*).

A major difficulty in formulating a valid molecular model of AvrRpt2 protease activation resides in the difficulty of achieving a clear separation of isomer-specific encounter complex formation and catalysis of prolyl isomerization (*28*).

The aim of this study was to elucidate the underlying molecular mechanism of AvrRpt2−cyclophilin complex-mediated proteolysis on a quantitative basis. We exploited the fact that prolyl isomerizations occur at relaxation times in the range of seconds to hours at room temperature (*29*, *30*). Thus, for thermodynamic reasons, AvrRpt2 activation via isomer-specific readjustment of prolyl bonds must lead to a delayed disappearance of proteolytic activity after the rapid dissociation of a functional AvrRpt2−cyclophilin−substrate complex. This fact should enable easy detection of the prolyl bond reisomerization in the time courses of a sufficiently sensitive proteolytic assay. Here, three complementary techniques, fluorescence-based steady state activity analyses, isothermal titration calorimetry, and far-UV CD measurements, were used to characterize the functional interaction of cyclophilins with AvrRpt2.

MATERIALS AND METHODS

Materials. Chemical reagents and solvents were purchased from Sigma Aldrich (Taufkirchen, Germany). The amino acid derivatives, coupling reagents, and resin were purchased from Novabiochem. The PPIase assay peptide Suc-AFPF-4-nitroanilide was purchased from Bachem (Weil, Germany).

Peptide Synthesis. Peptides were synthesized by solid-phase peptide synthesis with the Syro II robot (MultiSynTech, Witten, Germany) using 0.15 mmol Rink amide resin (100−200 mesh) (NovaBiochem, Läufelfingen, Switzerland). The preparations were created according to standard protocols for the Fmoc-protected amino acids. PyBOP/*N*-methylmorpholine (NovaBiochem) was used as the coupling reagent in dimethylformamide. Trifunctional amino acids were used as the side chain-protected derivatives carrying the following side chain protection: *tert*-butyl (tBu) for Glu and 3-nitro-Tyr (y) and *tert*-butyloxycarbonyl (Boc) for Trp. 2-Aminobenzoic acid was introduced as the Boc-protected derivative (Boc-Abz). A piperidine (20%)/DMF mixture was the standard cleavage cocktail used for Fmoc detachment. The resin was treated twice for 10 min. All couplings were performed using a 4-fold excess of the Fmoc amino acid derivative, PyBOP, and *N*-methylmorpholine in DMF. A double coupling protocol was used. After detachment of the peptides from the resins and side chain deprotection with a TFA/TIS/water mixture (95/3/2) at room temperature for 2 h, the crude peptides were precipitated with diethyl ether and purified by RP-HPLC on a Gilson 306 unit with a SP 250/10 Nucleosil 100-7 C8 column (Macherey-Nagel, Düren, Germany) using a water/acetonitrile (0.1% TFA) gradient. Purified peptides were lyophilized and stored at −20 °C. The purity of the peptides was evaluated by analytical HPLC using a LiChrospher 100, RP8, 5 μm, 125 mm × 4 mm column (LiChroCART Merck, Darmstadt, Germany) and a water/0.1% TFA/acetonitrile gradient from 5 to 100% over 30 min (flow rate of 1 mL/min). Detection was at 220 nm. The correct molecular masses were confirmed by MALDI-TOF mass spectrometry.

Proteins. Human Cyp18 was expressed from the pQE70-Cyp18 vector in *E. coli* M15 cells and purified as described previously (*31*). To obtain the expression plasmid of *Arabidopsis thaliana* His_6-ROC1, the gene was PCR-amplified using gene-specific primers from an ORF encoding *A. thaliana* ROC1 (imaGenes, Berlin, Germany), cloned into the NdeI and HindIII sites of pET28a, and overexpressed in *E. coli* BL21(DE3) cells. Purification of the His_6-tagged fusion protein was performed using affinity chromatography on Ni-NTA resin followed by size exclusion chromatography in 10 mM HEPES buffer (pH 7.8), 6 mM KCl, 1.5 mM $MgCl_2$, and 1 mM DTT. To obtain the expression plasmid of *E. coli* His_6-PPIB, the gene was PCR-amplified from *E. coli* genomic DNA with gene-specific primers, cloned into pET28a using NdeI and HindIII, and overexpressed in *E. coli* BL21(DE3) cells. Purification of the His_6-tagged fusion protein was performed using affinity chromatography on Ni-NTA resin. The His_6-PPIB-containing fractions were pooled, dialyzed against Tris buffer (10 mM, pH 8.0), and bound to a fractogel DEAE 650 matrix (Merck). Elution was performed with a linear gradient of up to 1 M NaCl. Finally, a size exclusion chromatography step was performed [10 mM HEPES buffer (pH 7.8), 6 mM KCl, 1.5 mM $MgCl_2$, and 1 mM DTT].

To obtain the expression plasmid of *P. syringae* His_6-AvrRpt2, the gene was PCR-amplified using gene-specific primers from the pV288 plasmid, which carries *P. syringae avrRpt2* (a kind gift of J. Boch, Halle, Germany), and cloned into the NdeI and BamHI sites of pET28a, yielding the pET28a-AvrRpt2 plasmid. The protein was overexpressed in *E. coli* BL21(DE3) cells. Purification and refolding were performed according to Coaker et al. (*5*). The truncated form of AvrRpt2 ($AvrRpt2^{72-255}$) was prepared by self-cleavage of His_6-AvrRpt2 on a preparative scale in the presence of 10 nM Cyp18 for 3 days at 25 °C in buffer [10 mM imidazole, 100 mM HEPES buffer (pH 7.5), 10 mM sodium bisulfite, 10 mM sodium metabisulfite, 500 mM NaCl, 10% glycerol, and 1 mM TCEP]. After dialysis in 100 mM HEPES buffer (pH 7.5), 10 mM sodium bisulfite, 10 mM sodium metabisulfite, 500 mM NaCl, and 10% glycerol, the His_6-$AvrRpt2^{1-71}$ was separated from $AvrRpt2^{72-255}$ by selective binding to Ni-NTA resin. The matrix-bound His_6-$AvrRpt2^{1-71}$ was eluted with 0.3 M imidazole in the buffer, purified by gel filtration, and stored at −20 °C for use. To avoid the risk of cyclophilin contamination of $AvrRpt2^{72-255}$, recombinantly expressed $AvrRpt2^{72-255}$ was produced and used in the long-term incubation experiment. Toward this end, the expression plasmid of *P. syringae* His_6-$AvrRpt2^{72-255}$ was generated by PCR amplification of the respective DNA fragment from the pET28a-AvrRpt2 plasmid using specific primers. The DNA fragment was cloned into the NdeI and BamHI sites of pET28. Overexpression of the protein was performed in *E. coli* BL21-(DE3) cells. Purification and refolding were performed as for the

full-length His_6-AvrRpt2 protein described above. The correct molecular masses were confirmed by MALDI-TOF mass spectrometry. Short-term proteolysis reactions, exemplified in Figure 5A, exhibited similar kinetics for both $AvrRpt2^{72-255}$ purified from the self-cleavage mixture and recombinatly expressed $AvrRpt2^{72-255}$.

Protease-Free PPIase Assay. Suc-AFPF-4-nitroanilide (~0.5 mg) was dissolved in 1 mL of anhydrous 0.55 M LiCl/TFE solvent mixture and stored at 4 °C. Solvent jumps were initiated by addition of the aliquot of a stock solution of peptide in a 0.55 M LiCl/TFE mixture into 35 mM HEPES buffer (pH 7.8) and 2.0 nM bovine serum albumin, resulting in a final peptide concentration of 64 μM at 10 °C. Absorbance at 390 nm was measured on an HP diode array spectrophotometer. A water-jacketed cell holder connected to a cryostat was used for temperature control. Monoexponential functions were fitted to the reaction progress curves. Assays were conducted in the presence and absence of a PPIase. Enzyme activities were calculated from the time course of the *cis*/*trans* isomerization by calculating first-order rate constants (k_{app}) with the relationship $k_{app} = k_0 + [E]k_{cat}/K_M$, where k_0 is the rate constant of the uncatalyzed reaction, [E] is the PPIase concentration, and k_{cat} and K_M are the turnover number and Michaelis constant, respectively. Care was taken to prevent protease contamination of assay constituents.

Prolyl isomerization of Abz-IEAPAFGGWy-NH_2 was monitored by utilizing the increase in fluorescence at 418 nm (excitation wavelength of 340 nm) when the *cis*/*trans* ratio decreases in aqueous buffer after a solvent jump from the stock solution in the 0.55 M LiCl/TFE mixture. The *cis*/*trans* isomerization was monitored at 10 °C with a Fluoromax 4 fluorescence spectrometer (Jobin-Yvon), and the temperature was controlled with a Peltier accessory.

Self-Cleavage of AvrRpt2. AvrRpt2 was incubated with cyclophilins in 50 mM phosphate buffer (pH 7.8), 10% glycerol, and 500 μM DTT at 20 °C. Aliquots (10 μL) of the reaction mixture were taken at several time points and used to monitor reaction progress by SDS−PAGE (15%) followed by Coomassie staining and densitometric quantification of the Coomassie-stained bands on a Scanmaker 1000XL (Microtek) using the band density software Multi-Analyst version 1.1 (Bio-Rad). AvrRpt2 protein was used as a standard.

Proteolytic Assay. For analysis of the proteolytic activity, decapeptides Abz-IEXPAFGGWy-NH_2 [X = A, L, or (D)A] and Abz-IEAXAFGGWy-NH_2 [X = (D)P or S] were used. In the original cleavage sequences of RIN4 and AvrRpt2, X is valine. Synthesis of the Val-containing Abz-IEVPAFGGWy-NH_2 peptide was accompanied by an impurity which interfered with some proteolytic experiments. Because $(k_{obs})_{valine}/(k_{obs})_{alanine} = 1.41$, activity differences were deemed small enough not to significantly affect proteolytic sensitivity. Fluorescence was monitored with a Fluoromax 4 fluorescence spectrometer (Jobin-Yvon) at 418 nm upon excitation at 320 nm. Typically, peptide hydrolysis was initiated by the addition of a stock solution of the peptide (1.0 mM) in DMSO into a semimicro fluorescence cell (d = 10 mm) containing 0.8 μM AvrRpt2 proteins and 8.0 μM cyclophilins in 35 mM HEPES buffer. The order of addition did not play a role in reaction kinetics. The final peptide concentration was 10 μM. Initial rates or complete first-order time traces were continuously recorded at 20.0 °C. To avoid prolonged dead times of mixing, a homemade mixing device was employed that allowed a mixing time of < 10 s without removal of the cell from the thermostated cell holder.

Parameters of the Michaelis−Menten equation for the proteolytic cleavage of the Abz-IEAPAFGGWy-NH_2 peptide by AvrRpt2/hCyp18 were obtained by determining initial rates of hydrolysis using RP-HPLC at various substrate concentrations. The assay mixture in 35 mM HEPES (pH 7.8) and 2.8% DMSO was thermostated at 10 °C for 10 min. After various time intervals (20, 60, 120, 180, and 240 s), 50 μL of the sample was withdrawn and the reaction was stopped by the addition of 2 μL of 0.5 mM CsA in a 50% H_2O/ethanol mixture. The samples were frozen immediately in liquid nitrogen and stored at −20 °C. The concentration of the cleavage product Abz-IEAPAFG-OH was quantified after separation by analytical HPLC using analysis of the peak area by fluorescence detection as described above. The initial rates of product formation (d[P]/dt) were calculated from the increase of the Abz-IEAPAFG-OH concentration over time and plotted against the respective substrate concentration.

Identification of cleavage sites in the fluorogenic peptides was conducted by ESI-MS (MSQ-Surveyor, Dionex) coupled to RP-HPLC (HPLC System, Dionex). Analytical separation of cleavage products was accomplished using various gradients of ACN (0.1% TFA) in H_2O (0.1%) on a Vydac RP8 (4.6 mm × 250 mm, 5 μm, Grace) or XTerra C18 (2.1 mm × 50 mm, 3.5 μm, Waters) column. Elution profiles resulted from monitoring at 220 nm.

CD Spectroscopy and ITC. Far-UV CD spectra were measured on a J-710 CD spectrometer (Jasco, Hellma, Germany) using a 0.1 mm quartz cell. All ITC experiments were conducted using a VP-ITC microcalorimeter from MicroCal (Northampton, MA) at the indicated temperature. All solutions were degassed for at least 5 min at the temperature used for the experiment. Reference titrations of buffer versus buffer and cyclophilins versus buffer were separately conducted and subtracted from the thermogram of the AvrRpt2−cyclophilin titrations.

RESULTS

Signature Protease Inhibitors Interfere with the Self-Cleavage of AvrRpt2. To determine whether proteolysis arises from a composite active site formed in the AvrRpt2−ROC1 complex consisting of the hidden serine protease triad constituents of cyclophilins (*32*) and the cysteine protease triad of AvrRpt2, we studied the time course of self-cleavage in the presence of a panel of protease inhibitors using ROC1 as the activator. The partial dispensability of the D226 residue in the putative cysteine protease catalytic triad of AvrRpt2 for proteolytic activity (*2*) suggests a contribution of an amino acid side chain of ROC1 in protease activation. Disappearance of the uncleaved AvrRpt2 in favor of $AvrRpt2^{72-255}$ after 300 min indicated uninhibited self-cleavage (Figure 1). Surprisingly, in the presence of E-64, a signature inhibitor of cysteine proteases, self-cleavage was not influenced. Similar results were found using serine and metalloprotease inhibitors except tosyl-Lys-chloromethylketone. Remarkably, several peptide aldehydes, including the proteasome inhibitor II and lactacystin, significantly inhibited proteolysis (data not shown).

Self-Cleavage of AvrRpt2 As Studied by Cyclosporin A Inhibition and Repetitive Substrate Dosing. To investigate whether the formation of $AvrRpt2^{72-255}$ in the course of self-cleavage of AvrRpt2 results in a cyclophilin-independent proteolytic activity, we performed a double-jump experiment consisting of a delayed addition of cyclosporin A (CsA) following the initiation of the reaction by hCyp18. CsA is a tight binding cyclophilin inhibitor inherently able to displace bound AvrRpt2 from the active site of the PPIase. Upon delivery of CsA, the

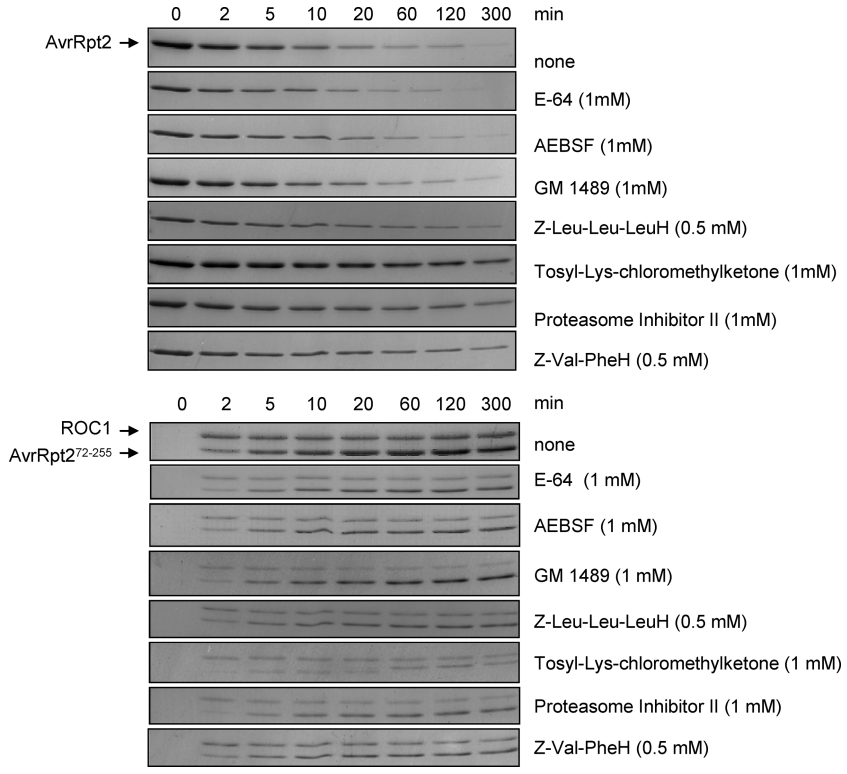

FIGURE 1: Pharmacological inhibition of the self-cleavage of AvrRpt2 in the presence of ROC1. AvrRpt2 (4.0 μM) and ROC1 (2.0 μM) were incubated with or without the indicated inhibitors at 20 °C in 50 mM potassium phosphate buffer (pH 7.8), 500 mM DTT, and 10% glycerol. Equal sample volumes (10 μL) were taken at various time points, mixed with Laemmli buffer, and boiled for 5 min at 95 °C; 15% SDS−PAGE gels were run and stained with Coomassie blue.

kinetics of the proteolytic reaction were expected to indicate whether an altered *cis*/*trans* ratio of functionally important proline residues exists for the Michaelis complex. Self-cleavage abruptly stopped after CsA addition and after a significant amount of AvrRpt2$^{72-255}$ (Figure 2) had been formed. Using isothermal titration calorimetry (ITC), CsA was shown to exhibit exclusive affinity for hCyp18 (*31*), leaving AvrRpt2 unbound (Figure S2C of the Supporting Information).

To further analyze whether the formation of AvrRpt2$^{72-255}$ in the course of self-cleavage of AvrRpt2 can give rise to an altered proteolytic activity, we restarted the reaction cycle with a new batch of AvrRpt2 after it was fully consumed in the first reaction cycle. If self-cleavage would contribute to an activation process involving AvrRpt2 protease maturation, a higher rate would be expected for higher cycle numbers. However, as shown in Figure 3, the self-cleavage rate did not change in response to a 4-fold increase in the level of AvrRpt2$^{72-255}$ in the presence of a constant concentration of ROC1. The same experiment conducted in the presence of hCyp18 produced similar results (data not shown). Autocatalysis of self-cleavage can thus be ruled out. Product inhibition by AvrRpt2$^{1-71}$ could also explain the decreased self-cleavage rate when AvrRpt2$^{72-255}$ accumulated. Alternatively, an intramolecular reaction mode of self-cleavage (*3*) would make the AvrRpt2−cyclophilin complex the only productive species, rendering the reaction rate independent of AvrRpt2$^{72-255}$ accumulation. To answer this question, we developed a fluorescence-based oligopeptide assay that would enable us to continuously monitor proteolytic cleavage at a higher time resolution.

AvrRpt2-Derived Decapeptide Substrates Allow Quantification of Proteolytic Cleavage. The positional specificity of the proteolytic reactions described above probably ranges

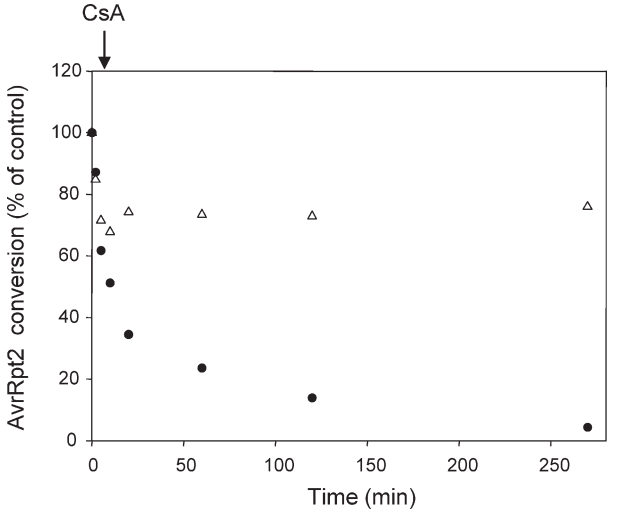

FIGURE 2: Double-jump experiment with CsA in the ongoing AvrRpt2 self-processing reaction. Time course of the self-cleavage of an AvrRpt2 (4.0 μM)/ROC1 (2.0 μM) mixture with a 5 min delay of delivery of CsA (20 μM) (arrow) after the reaction was started by ROC1. The decrease in the AvrRpt2 band intensity in the SDS−PAGE gel was used to quantify self-cleavage. The time course with CsA is indicted with triangles, and the reference reaction without CsA is shown with circles. Experimental conditions are provided in the legend of Figure 3.

from amino acid 67 to 73 of AvrRpt2 and from site I amino acid 6 to 12 and site II amino acid 148 to 154 of RIN4, respectively (*1*−*3*). To take advantage of this array of subsites, we synthesized fluorescence-quenched (*33*) decapeptides (Abz-IEXPAFGGWy-NH_2, X = A or L, and y = 3-nitrotyrosine), which represent derivatives of the AvrRpt2 cleavage sites mentioned

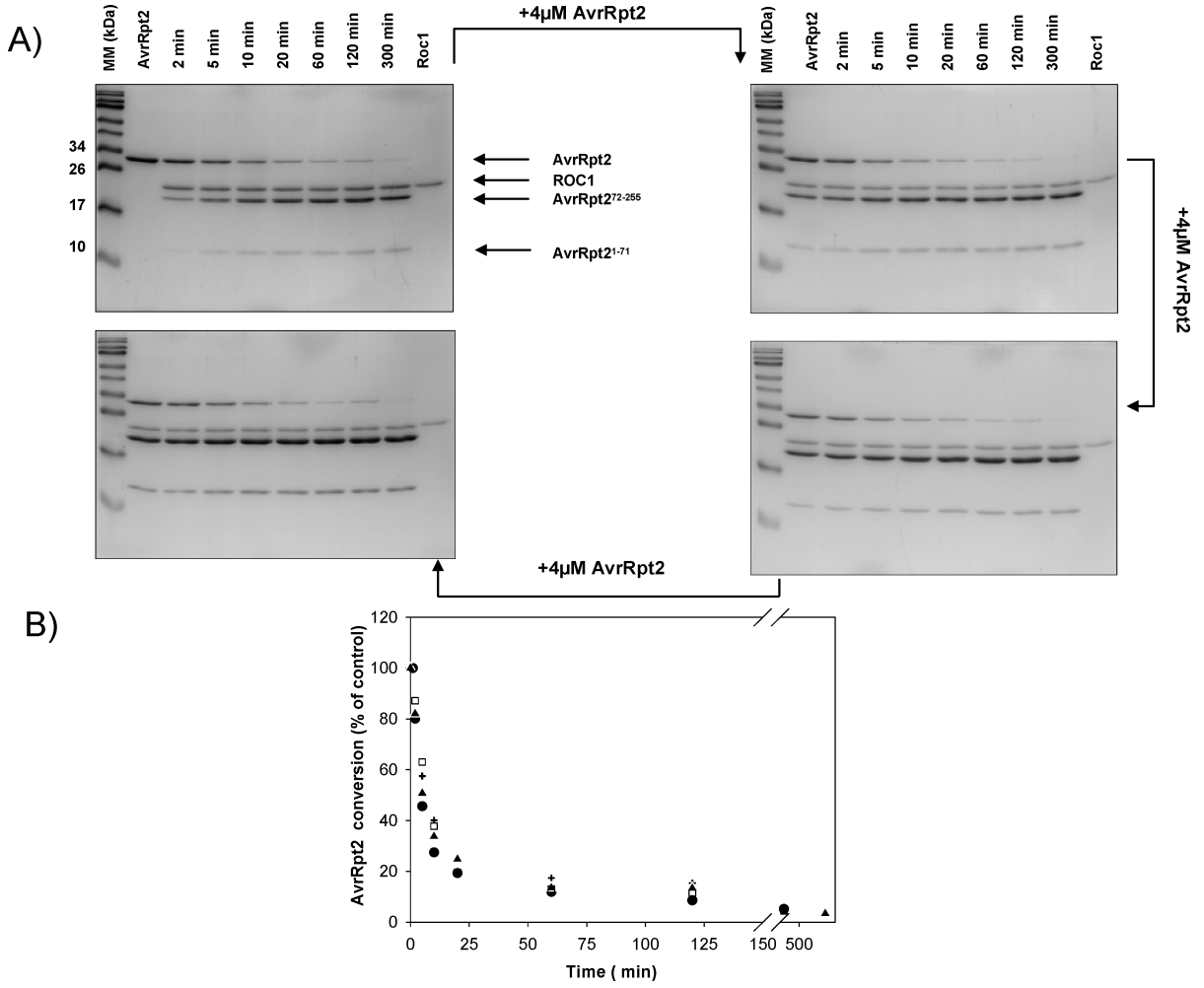

FIGURE 3: Time courses for the self-cleavage of AvrRpt2 in the presence of ROC1 (2.0 μM) with repetitive delivery of AvrRpt2. (A) AvrRpt2 (4.0 μM) was incubated with ROC1. After completion of AvrRpt2 cleavage (300 min), the reaction mixture was restarted by delivery of a new portion of AvrRpt2 (4.0 μM). Delivery of AvrRpt2 was repeated three times, and time courses were followed until the reaction was complete. (B) Densitometry was used to compare the relative intensities of the AvrRpt2 bands in the dependence on reaction time for the repetitive cycles of reactant delivery. Gel background correction was applied: first cycle (+), second cycle (▲), third cycle (●), and fourth cycle (□).

above. HPLC−ESI-MS experiments were performed to detect the proposed hydrolysis products (Figure 4A). Exclusive cleavage between Gly and Gly was detected in the presence of AvrRpt2 and ROC1 (or hCyp18), indicating qualitative similarity of self-processing and intermolecular decapeptide substrate cleavage. Incubation of the decapeptide with AvrRpt2 or AvrRpt2$^{72-255}$ alone revealed complete stability with no sign of any product peak even after a prolonged incubation time of 288 h (Figure 4C). In addition, a similar experiment performed in the sole presence of ROC1 did not show any trace of a product peak (Figure 4B). The detection limit of the experiment depicted in Figure 4C indicated that the hCyp18-mediated rate enhancement amounted to more than 10^5-fold.

Importantly, the protease reaction could be continuously monitored because the drop in 3-nitrotyrosine-mediated Abz quenching after substrate hydrolysis caused an ~6-fold increase in fluorescence at 418 nm. At a substrate concentration of 10 μM, AvrRpt2$^{72-255}$/hCyp18-catalyzed hydrolysis was a strict first-order process over the whole time course, which was demonstrated by the equally distributed residuals around the zero level (Figure 5A). Thus, calculated first-order rate constants (k_{obs}) of the progress curves at a substrate concentration of 10 μM were directly proportional to the k_{cat}/K_M of proteolysis. This observation is consistent with the K_M value of 140 ± 23 μM and the V_{max} of 35 ± 3.0 nM s^{-1} measured by the standard concentration dependence of the initial rates of product formation of Abz-IELPAFGGWy-NH_2. For this purpose, we used time-dependent HPLC analysis of the AvrRpt2$^{72-255}$/hCyp18/decapeptide mixture (Figure S1 of the Supporting Information). The first-order rate constants indicated a 2.5-fold higher specificity constant of Abz-IELPAFGGWy-NH_2 when compared with that of Abz-IEAPAFGGWy-NH_2. Remarkably, the preference of Leu over Ala is at the P5 subsite.

The sensitivity of the assay permitted us to compare the potential for AvrRpt2 activation of hCyp18, *E. coli*PPIB, and ROC1 (Table 1). Substrates were hydrolyzed, with hCyp18 as the most efficient AvrRpt2$^{71-255}$-activating cyclophilin. However, the rate constants of proteolysis did not correspond with PPIase activities measured in a standard PPIase assay and in the decapeptide PPIase assay. Although all three cyclophilins catalyzed prolyl isomerization in the decapeptide powerfully, *E. coli* PPIB was not able to significantly support the proteolytic reaction. Compared with that of ROC1, the higher sensitivity of the hCyp18-assisted proteolysis renders it more suitable to kinetic investigations.

To calculate the possibility of altered proteolytic activity upon self-cleavage, AvrRpt2$^{72-255}$ and AvrRpt2 were directly compared in the decapeptide assay over a broad time range (Figure 5B).

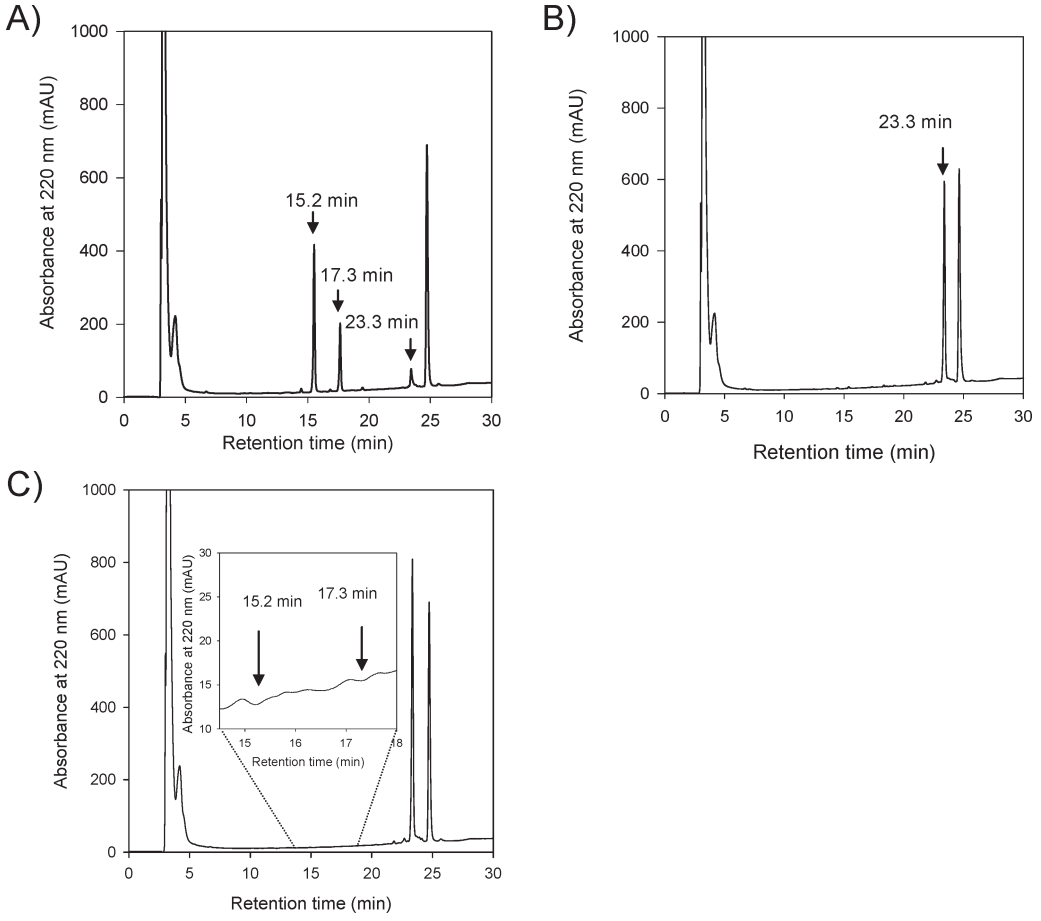

FIGURE 4: Identification of the cleavage site in Abz-IEAPAFGGWy-NH_2. (A) HPLC profile of 50 μM Abz-IEAPAFGGWy-NH_2 after overnight incubation with 1.0 μM recombinantly produced AvrRpt2$^{72-255}$ and 10 μM ROC1 in 35 mM HEPES buffer (pH 7.8) and 0.1% sodium azide at room temperature. The substrate peptide elutes at 23.3 min (MW of 1273.3 g/mol, m/z 1273.4). After proteolytic cleavage, the two cleavage products, Abz-IEAPAFG-OH (retention time of 17.2 min, MW of 822.9 g/mol, m/z 823.2) and H-GWy-NH_2 (retention time of 15.2 min, MW of 468.4 g/mol, m/z 469.1), were identified by ESI-MS. The peak at 24.5 min results from AvrRpt2$^{72-255}$ and ROC1 elution. (B) Long-term incubation experiment of Abz-IEAPAFGGWy-NH_2 with ROC1 (10 μM) alone under the conditions used for panel A. At the incubation time of 288 h, no trace of a product peak at 15.2 and 17.3 min is detectable. (C) Long-term incubation experiment for Abz-IEAPAFGGWy-NH_2 with recombinantly produced AvrRpt2$^{72-255}$ (1.0 μM) alone under the conditions used for panel A. The lacking product peaks (inset) indicate < 1% product formed after incubation for 288 h.

The absence of any detectable deviation from the simple first-order rate law in the course of continuous production of AvrRpt2$^{72-255}$ and the simultaneouse depletion of AvrRpt2 during self-cleavage indicate identical kinetic behavior of the two AvrRpt2 species. Furthermore, direct comparison of initial rates by stopped-flow mixing confirmed that AvrRpt2/hCyp18 and AvrRpt2$^{72-255}$/hCyp18 mixtures exhibited similar catalytic activities (Figure 5B, inset).

Under the conditions used in the experiment (Figure 5A), the reaction product AvrRpt2$^{1-71}$ was formed stoichiometrically along with AvrRpt2$^{72-255}$ from AvrRpt2 within the time course of decapeptide hydrolysis. The inhibitory capacity of AvrRpt2$^{1-71}$ for ROC1- and hCyp18-assisted proteolysis was determined with IC_{50} values of 36 ± 12 and 7.0 ± 0.5 μM, respectively. We avoided inhibition by AvrRpt2$^{1-71}$ during reaction progress by using low initial concentrations of AvrRpt2. The fluorometric assay also permitted us to determine an IC_{50} value 88.4 ± 7 nM for CsA in the proteolytic reaction (Figure S5 of the Supporting Information). This value is within the range of the inhibition constants reported for the binary CsA−hCyp18 interaction (*31*).

Assistance by Cyclophilins Is Not at the Level of Substrate Activation. Previous findings showed that many proteases can discriminate against a *cis* prolyl bond in the substrate and that discrimination can be kinetically resolved by cyclophilin catalysis. Therefore, we investigated whether the P4 position of a substrate is a critical determinant for cyclophilin assistance and for the cleavage at the GG site by using the decapeptides Abz-IEAXAFGGWy-NH_2 [X = P, S, or (D)P] and Abz-IEXPAFGGWy-NH_2 [X = A or (D)A]. Replacement of the P4 proline with a serine residue would virtually eliminate a backbone *cis* conformation in the decapeptide (*34*) and would also remove a potentially important (*35*) subsite interaction. In addition, the various substitutions should increase resistance toward cyclophilin PPIase function (*36*). Comparisons of proteolysis rates were made between these substrates under similar reaction conditions on the basis of first-order rate constants (k_{obs}) characterized above. A reduced capability to undergo self-cleavage has already been shown for the AvrRpt2 P68A variant (*14*). In the decapeptide assay, a k_{obs}(AP)/k_{obs}(AS) ratio of 166 was observed along with an unchanged GG cleavage site (Figure S6 of the Supporting Information). This indicates that proline is involved in catalytically important subsite interactions at the protease site. Alternatively, the lack of PPIase catalysis might play the major role. To resolve this issue, enantiomeric substitutions of AP with (D)AP or A(D)P in the decapeptide substrate were used. With these substitutions in the standard decapeptide substrate, hCyp18

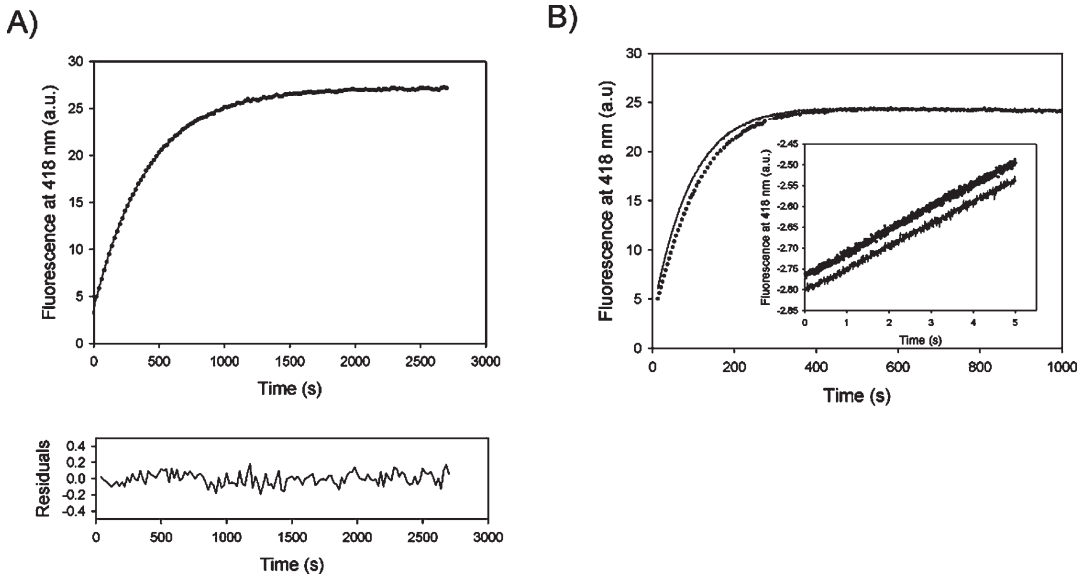

FIGURE 5: (A) Time course of the cleavage of Abz-IEAPAFGGWy-NH_2 (10 μM) monitored at 418 nm in the presence of hCyp18 (49.8 nM) and AvrRpt2$^{72-255}$ (80 μM) (●) and calculated curve using a first-order rate constant k_{obs} of 2.44×10^{-3} s^{-1} (—). Residuals of the calculation are shown in the bottom panel. (B) AvrRpt2 and AvrRpt2$^{72-255}$ exhibit similar proteolytic activity toward Abz-IEAPAFGGWy-NH_2 (10 μM) when activated by hCyp18. In the presence of hCyp18 (8.2 μM), AvrRpt2 (0.8 μM) and AvrRpt2$^{72-255}$ (0.8 μM) hydrolyze the substrate with k_{obs} values of 0.0101 (···) and 0.0115 s^{-1} (—), respectively. The inset shows stopped-flow kinetics in the presence of hCyp18 (6.3 μM). With Abz-IELPAFGGWy-NH_2 (16.3 μM) as the substrate, AvrRpt2 (0.93 μM) and AvrRpt2$^{72-255}$ (0.93 μM) display the following initial rates: $v = 0.534$ ΔF_{418} s^{-1} (···) and $v = 0.551$ ΔF_{418} s^{-1} (—), respectively.

Table 1: Rate Constants of the Proteolysis and Prolyl Isomerization in the Presence of Cyclophilins at pH 7.8

cyclophilin	k_{obs} (s^{-1}) (proteolysis)[a]	k_{cat}/K_M (M^{-1} s^{-1}) (-FPF- isomerization)[b]	k_{cat}/K_M (M^{-1} s^{-1}) (-APA- isomerization)[c]
hCyp18	6.70×10^{-3}	1.28×10^{7}	2.49×10^{6}
ROC1	1.18×10^{-3}	4.50×10^{6}	1.24×10^{6}
E. coli PPIB	1.01×10^{-6}	4.70×10^{6}	2.35×10^{6}

[a]First-order rate constants (k_{obs}) of the cleavage between Gly residues of Abz-IEAPAFGGWy-NH_2 (10 μM) catalyzed by AvrRpt2$^{72-255}$ (0.8 μM) and cyclophilins (7.98 μM) at 20 °C. [b]Second-order rate constants (k_{cat}/K_M) of the cyclophilin-catalyzed reversible *cis*/*trans* isomerization of Suc-AFPF-4-nitroanilide at pH 7.8 and 10 °C. [c]Second-order rate constants (k_{cat}/K_M) of the cyclophilin-catalyzed reversible *cis*/*trans* isomerization of Abz-IEAPAFGGWy-NH_2 at pH 7.8 and 10 °C. Values result from three independent measurements. Standard deviations of the kinetic constants did not exceed 10%.

is expected to be a very inefficient isomerization catalyst (*37*). A comparison of peptide proteolysis kinetics of those to the AP-containing decapeptide suggested k_{obs} ratios of 12.5 and 62.5, respectively.

Given the 2.5-fold difference in k_{obs} values for the exchange of LP for AP, the slightly stronger influence of enantiomeric substitutions on proteolytic efficiency is probably not related to the activation mechanism itself. It might indicate contributions of the subsite to the transition state stabilization of the already activated protease. In fact, the magnitude of the effects is comparable to those found for enantiomeric discrimination factors of catalytically important subsites in the other proteases (*38*). Collectively, the findings indicated that an effect of a cyclophilin on the isomerization of the prolyl bond at the P4 subsite is not a critical determinant for induction of peptide bond hydrolysis.

Functional Relevance of the Equilibrium cis/*trans Ratio in AvrRpt2$^{72-255}$.* We next investigated whether cyclophilins could contribute to controlling the AvrRpt2 fold, thereby ensuring the proteolytically active state with a *cis* prolyl bond in the molecule (*6*). If cyclophilins would change the *cis* prolyl bond propensity in AvrRpt2, the proteolytically active state of AvrRpt2 must be transiently or permanently retained upon addition of CsA into an ongoing proteolytic reaction of the substrate peptide. The relaxation of the intrinsically slow *cis*/*trans* prolyl isomerization would translate into a slowly decreasing rate or even to complete preservation of proteolysis. Double-jump experiments with CsA were performed on the $10^{-3}-t-10^{3}$ second time scale (Figure 6). Results implied that CsA completely blocked ongoing proteolysis with no sign of kinetic transients occurring after the dead time of mixing of 1.5 ms. The lack of slow kinetic phases is inconsistent with the hypothesis of cyclophilin-induced alterations of the *cis*/*trans* ratio of prolyl bonds in the activation of AvrRpt2$^{72-255}$.

Far-UV Difference Spectra Reveal Structural Similarities of Free AvrRpt2$^{72-255}$ and the AvrRpt2$^{72-255}$−ROC1 Complex. Given the potent activating interaction of cyclophilins with AvrRpt2 characterized by a $>10^{5}$-fold rate enhancement, one might envisage profound secondary structure changes in the AvrRpt$^{272-255}$−cyclophilin complexes. Indeed, NMR studies and gel filtration chromatography have revealed extensive structure formation in the presence of GST-fused ROC1 (*6*). Therefore, a direct comparison of far-UV CD spectra of the proteins in complex and in isolation was performed. For these measurements, we needed to ensure a nearly complete formation of the AvrRpt2$^{72-255}$−cyclophilin complex at the experimental protein concentrations of the CD measurements. ITC was used to characterize the thermodynamics of formation of the AvrRpt2$^{72-255}$–ROC1 and AvrRpt2$^{72-255}$−hCyp18 complexes (Figures S2 and S3 of the Supporting Information). Similar binding isotherms were found for hCyp18 and ROC1 with K_{diss} values of 16.4 and 16.1 μM, respectively. Notably, an additional binding site was titrated for the ROC1 complex ($K_{diss} = 0.17$ μM). To identify the probability of higher-order complexes in the presence of a protease substrate, we generated Job plots for the formation of

functional AvrRpt2$^{72-255}$–cyclophilin complexes. Here, the first-order rate constants of hydrolysis were measured by continuous variation of the mole fraction of the components while the total protein concentration remained constant (Figure S5 of the Supporting Information). The asymmetric curves indicated the simultaneous presence of binary complexes and higher-order molecular complexes with both types of cyclophilins, but quantitative description by an interaction model could not yet be achieved. On the basis of these binding data, far-UV CD spectra were recorded using ROC1 and AvrRpt2$^{72-255}$ (50 μM each) in isolation or in a mixture (Figure 7). Under these conditions, more than 90% of the proteins existed in complexes. Essentially, the overlay of the spectra and the difference spectrum indicated interaction relevant spectral changes near the zero level throughout the spectral range (Figure 7C). A similar result was found for the hCyp18/AvrRpt2 mixture (data not shown). Interestingly, compared with the far-UV CD spectra of AvrRpt2$^{72-255}$, those of AvrRpt2 did not show marked changes, supporting the idea of functional similarity and congruent native state folds of both proteins (Figure S4 of the Supporting Information).

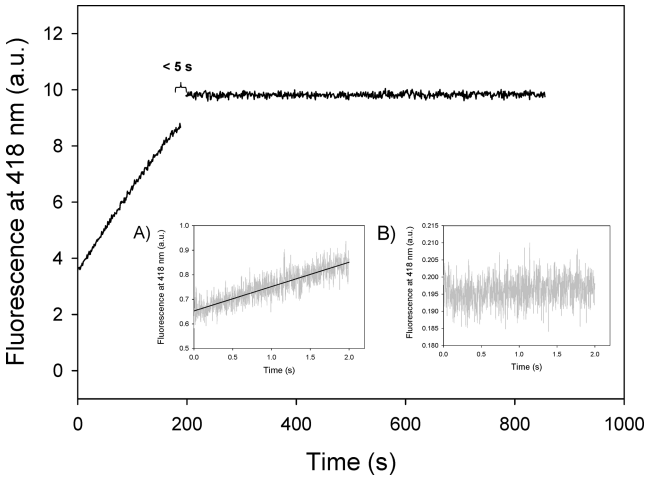

FIGURE 6: Double-jump CsA inhibition experiments. CsA (19.6 μM) was injected into a mixture of Abz-IEAPAFGGWy-NH_2 (10 μM) and hCyp18 (0.9 μM) with AvrRpt2$^{72-255}$ (1.0 μM) 188 s after the initiation of the cleavage reaction in 35 mM HEPES buffer (pH 7.8) at 20 °C. The insets present stopped-flow double-jump measurements of substrate proteolysis inhibited by CsA. The time course of fluorescence of Abz-IELPAFGGWy-NH_2 was followed after stopped-flow mixing of hCyp18 (6.0 μM) and substrate (4.0 μM) in one syringe with AvrRpt2$^{72-255}$ (2.3 μM) followed by a 20 μM CsA concentration jump after a 0.991 s reaction time (inset B). Data for the noninhibited reference reaction are shown in inset A. Final concentrations are indicated.

DISCUSSION

The putative cysteine protease AvrRpt2 has the unique ability of increasing its proteolytic power by more than 10^5-fold upon noncovalent interaction with activator cyclophilins, resulting in generation of a robust hydrolytic enzyme. The binary AvrRpt2–hCyp18 complex was the most productive species under the conditions tested, with the turnover number for Abz-IEL-PAFGGWy-NH_2 cleavage calculated to be 3.5 ± 0.4 s^{-1}. As turnover numbers for the GG cleavage of a panel of hexapeptide substrates by papain lie in the range of 2.7–28 s^{-1} (*32*), the proteolytic capacity of the AvrRpt2/hCyp18 mixture can be considered to be similarly potent. We also note that there is good reason to hypothesize that AvrRpt2 in isolation is nearly inactive when probed with the PAFGGW substrate sequence (Figure 4C, inset). In this respect, this reaction provides the long-sought evidence supporting the idea of a PPIase-mediated on–off switch of a biologically relevant signal (*39*). We conclude, therefore, that the proteolysis of substrates catalyzed by an AvrRpt2 species stringently requires the permanent presence of an activating cyclophilin.

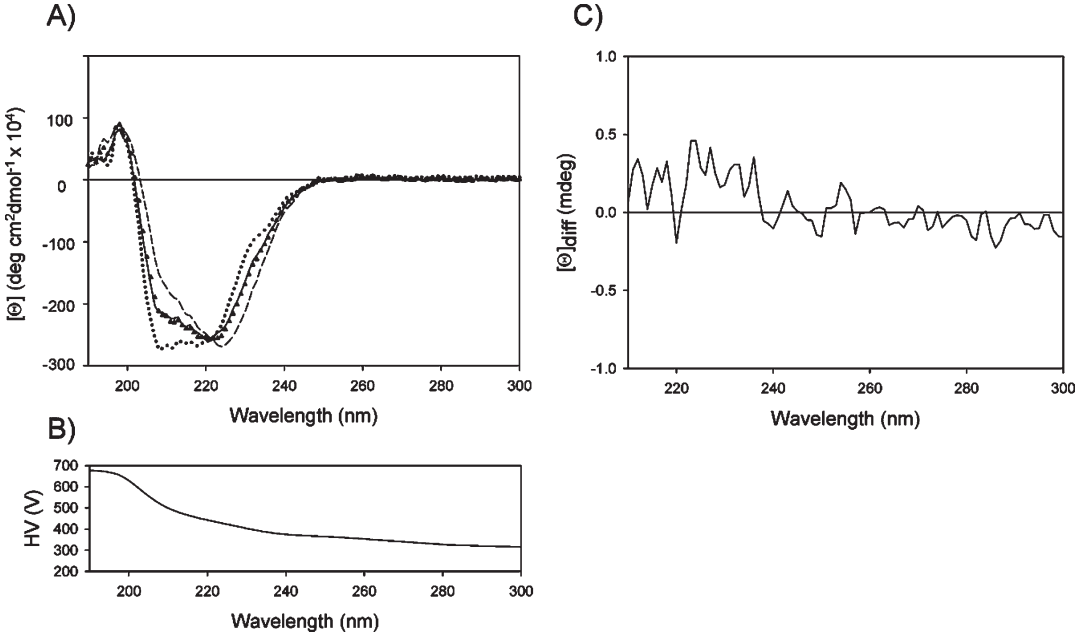

FIGURE 7: (A) Far-UV CD spectra of AvrRpt2$^{72-255}$ [d = 0.1 mm (+)] and ROC1 [d = 0.1 mm (– – –)], both at 100 μM, calculated sum of the spectra of both proteins in isolation at 50 μM each [d = 0.1 mm (—)], and experimental far-UV CD spectrum of a 1/1 mixture of both proteins [d = 0.1 mm (△)] at 50 μM. The molar ellipticity is plotted vs the wavelength. (B) Wavelength-dependent recording of the high voltage of the PM tube. (C) Difference spectrum [$[\Theta]_{diff}$ (in millidegrees) = $[\Theta]_{free} - [\Theta]_{mixture}$]. A constant temperature of 20.0 °C and a path length of 0.1 mm were maintained. Proteins were dissolved in 50 mM phosphate buffer (pH 7.4) containing 10% gycerol. Buffer reference was subtracted from the curves.

Rate enhancement of proteolysis by external factors can be found for proteases where an incomplete active site is complemented by a polypeptide ligand as exemplified in retroviral protease homodimerization (*43*). Recruitment of cyclophilin amino acid side chains of cyclophilins by AvrRpt2 might be a reason for the high rate enhancement factor. In this light, the finding that an inactive catalytic triad of a serine protease exists in hCyp18 (*31*) and possibly in ROC1 (suggested by sequence alignment), but not in the nonactivating PPIase *E. coli* PPIB (Table 1), may be significant. On the other hand, an *E. coli* PPIB triple mutant protein was identified as a moderately active proline-specific endopeptidase of the serine protease type (*40*). Inhibition experiments were expected to be indicative of the participation of hCyp18 in the formation of a proteolytic site. Neither the epoxide cysteine protease inactivator E-64 nor the active site serine-directed compound AEBSF was found to diminish self-cleavage of AvrRpt2. Unexpectedly, inhibitors of the chymotrypsin-like activity of the proteasome such as proteasome inhibitor II (Figure 1), lactacystin, and expoximicin (data not shown) could be identified as inhibitors in the self-cleavage assay and in decapeptide proteolysis. We interpreted the lack of E-64 inhibition as steric hindrance of E-64 binding similar to the case reported for another staphopain-related cysteine protease, the ataxin-3 Jospehin domain (*41*). We noted that the thiol anion-directed papain inhibitor tosyl-Lys-chloromethylketone (*42*), which does not inhibit chymotrypsin-like activities, also decreased the rate of self-cleavage of AvrRpt2. In our inhibition experiments, however, the participation of the hidden catalytic serine protease triad of cyclophilins in the assisted self-cleavage of AvrRpt2 could not be assessed.

Considerable rate enhancements of proteolytic reactions have also been found for processing zymogens to mature proteases (*44*) or for binding to highly specific plasminogen activators (*45*). The self-cleavage of AvrRpt2 producing AvrRpt2$^{72-255}$ formally resembles the molecularity of zymogen activation. However, our results clearly indicate that AvrRpt2 self-cleavage in the presence of cyclophilins does not lead to a more potent proteolytic enzyme when assayed with Abz-IELPAFGGWy-NH_2. In summary, AvrRpt2 cannot be termed a proenzyme, the product of self-cleavage (AvrRpt2$^{72-255}$) is not active in isolation, and AvrRpt2 and AvrRpt2$^{72-255}$ are equally susceptible to cyclophilin activation.

A combination of proteolytic activation by formation of a new N-terminus and activating conformational interconversion has been demonstrated for the complement system (*46*). The serine protease triad of factor D is blocked by a self-inhibitory loop, which can be released from the catalytic center by a specific substrate, C3b-bound factor B (*47*). Our attempt to identify by far-UV CD spectroscopy structural differences between AvrRpt2$^{72-255}$ in isolation and in AvrRpt2$^{72-255}$−cyclophilin complexes was unsuccessful. Having quantitatively described the formation of AvrRpt2$^{72-255}$−cyclophilin complexes by ITC, we were then able to probe prolyl bonds for transient or permanent conformational alterations upon formation of AvrRpt2$^{72-255}$−cyclophilin complexes. In double-jump experiments with CsA, the absence of kinetic transients indicated a lack of correlation between proteolytic reaction and the increased *cis*/*trans* isomer ratio of functionally relevant AvrRpt2$^{72-255}$ prolyl bonds. Furthermore, activation of the substrate by cyclophilin-assisted *cis*/*trans* isomerization at the P4 proline subsite cannot serve as a molecular basis of the cyclophilin effects. In the decapeptide assay, the *cis*/*trans* ratio of the substrate is not far from unity, thus providing sufficient reactive isomer for the proteolytic reaction without the need for cyclophilin assistance. Consistent with this view, decapeptide substrates carrying enantiomeric substitutions such as the (D)Pro residue abolish cyclophilin catalysis of prolyl isomerization (*37*) but do not completely abrogate the protease reaction. In addition, the effect of *E. coli* PPIB enabled a clear distinction between targeting a prolyl bond of a substrate for isomerization, which was detectable, and targeting a prolyl bond of an AvrRpt2 species for activating the protease function, which could not be observed. This result likely excludes the classical pathway of isomer-specific proteolysis illustrated by the lack of *cis* substrate recognition by the protease. A proline residue is thus preferred at P4 of the substrate without a specific requirement for either the *cis* isomer or the *trans* isomer of the prolyl bond for induction of proteolysis.

To further limit the scope of possible catalytic models to be considered, reaction progress curves were analyzed. The missing pre-steady state product burst demonstrated that the cyclophilins do not accelerate a reaction step following a single turnover but rather that acyl enzyme formation is activated. Among the cyclophilins tested, hCyp18 is 5.7- and 6.6×10^3-fold more activating than ROC1 and *E. coli* PPIB, respectively. This finding does not link protease activation to a general PPIase activity because the specificity constants (k_{cat}/K_M) for the *cis* to *trans* isomerization of the Xaa-Pro PPIase substrates are rather similar (Table 1). On the other hand, a lack of activation was reported for the PPIase-inactive GST−ROC1 R62A variant (*6*). However, this result does not unequivocally prove the importance of PPIase catalysis in AvrRpt2 activation because the Arg62Ala substitution not only corrupted catalysis but also influenced the affinity for proline-containing polypeptide chains (*18*). Nevertheless, from these data, we could infer that the polypeptide binding ability of the active site of cyclophilins plays a crucial role in the rate enhancement of proteolysis. It indicates that the binary AvrRpt2−cyclophilin complex is either the protease-active Michaelis complex of the PPIase reaction or an encounter complex (*28*) presenting a correctly positioned catalytic triad to the substrate.

In conclusion, we believe that cyclophilin-dependent activation reaction of AvrRpt2$^{72-255}$ constitutes a powerful tool for a more thorough characterization of PPIase-induced on−off switches in biological signaling. Proteolytic activation does not involve isomer specificity in substrate recognition or cyclophilin-induced alterations in the *cis*/*trans* ratio or even alterations in the general fold of AvrRpt2. In spite of some compelling indirect evidence, a clear role for prolyl isomerizations in the AvrRpt2 activation by cyclophilins has not yet been established. In light of the large rate enhancement factor for a noncovalent interaction, this problem is of particular importance in biocatalysis and remains the focus of our research.

ACKNOWLEDGMENT

We thank Suzanne Ross, Dirk Tänzler, and Barbara Korge for excellent technical assistance and David Ferrari for critical reading of the manuscript. We are grateful to Petr Kuzmic (Watertown) for helpful discussions.

SUPPORTING INFORMATION AVAILABLE

Michaelis−Menten plot for the proteolysis of Abz-IEAPAFGGWy-NH_2 along with analysis of the hydrolysis products, isothermal titration calorimetry of AvrRpt2$^{72-255}$−cyclophilin

interactions, the far-UV CD spectrum of AvrRpt2, Job plots for the hydrolysis of Abz-IEAPAFGGWy-NH_2 by AvrRpt2$^{72-255}$/cyclophilin mixtures, and the activity−concentration dependence for the inhibition of the proteolytic reaction by cyclosporin A. This material is available free of charge via the Internet at http://pubs.acs.org.

REFERENCES

1. Mudgett, M. B., and Staskawicz, B. J. (1999) Characterization of the *Pseudomonas syringae* pv. tomato AvrRpt2 protein: Demonstration of secretion and processing during bacterial pathogenesis. *Mol. Microbiol. 32*, 927–941.
2. Axtell, M. J., Chisholm, S. T., Dahlbeck, D., and Staskawicz, B. J. (2003) Genetic and molecular evidence that the *Pseudomonas syringae* type III effector protein AvrRpt2 is a cysteine protease. *Mol. Microbiol. 49*, 1537–1546.
3. Jin, P., Wood, M. D., Wu, Y., Xie, Z. Y., and Katagiri, F. (2003) Cleavage of the *Pseudomonas syringae* type III effector AvrRpt2 requires a host factor(s) common among eukaryotes and is important for AvrRpt2 localization in the host cell. *Plant Physiol. 133*, 1072–1082.
4. Hotson, A., and Mudgett, M. B. (2004) Cysteine proteases in phytopathogenic bacteria: Identification of plant targets and activation of innate immunity. *Curr. Opin. Plant Biol. 7*, 384–390.
5. Coaker, G., Falick, A., and Staskawicz, B. (2005) Activation of a phytopathogenic bacterial effector protein by a eukaryotic cyclophilin. *Science 308*, 548–550.
6. Coaker, G., Zhu, G., Ding, Z. F., Van Doren, S. R., and Staskawicz, B. (2006) Eukaryotic cyclophilin as a molecular switch for effector activation. *Mol. Microbiol. 61*, 1485–1496.
7. Romano, P. G. N., Horton, P., and Gray, J. E. (2004) The *Arabidopsis* cyclophilin gene family. *Plant Physiol. 134*, 1268–1282.
8. Kaul, A., Stauffer, S., Berger, C., Pertel, T., Schmitt, J., Kallis, S., Lopez, M. Z., Lohmann, V., Luban, J., and Bartenschlager, R. (2009) Essential role of cyclophilin A for hepatitis C virus replication and virus production and possible link to polyprotein cleavage kinetics. *PLoS Pathog. 5*, e1000546.
9. Wagner, C., Khan, A. S., Kamphausen, T., Schmausser, B., Unal, C., Lorenz, U., Fischer, G., Hacker, J., and Steinert, M. (2007) Collagen binding protein Mip enables *Legionella pneumophila* to transmigrate through a barrier of NCI-H292 lung epithelial cells and extracellular matrix. *Cell. Microbiol. 9*, 450–462.
10. Fischer, G., and Aumüller, T. (2003) Regulation of peptide bond *cis*/*trans* isomerization by enzyme catalysis and its implication in physiological processes. *Rev. Physiol. Biochem. Pharmacol. 148*, 105–150.
11. Schechter, I., and Berger, A. (1967) On the size of the active site in proteases. I. Papain. *Biochem. Biophys. Res. Commun. 27*, 157–162.
12. Lin, L. N., and Brandts, J. F. (1985) Isomer-specific proteolysis of model substrates: Influence that the location of the proline residue exerts on *cis*/*trans* specificity. *Biochemistry 24*, 6533–6538.
13. Fischer, G., Bang, H., Berger, E., and Schellenberger, A. (1984) Conformational specificity of chymotrypsin toward proline-containing substrates. *Biochim. Biophys. Acta 791*, 87–97.
14. Chisholm, S. T., Dahlbeck, D., Krishnamurthy, N., Day, B., Sjolander, K., and Staskawicz, B. J. (2005) Molecular characterization of proteolytic cleavage sites of the *Pseudomonas syringae* effector AvrRpt2. *Proc. Natl. Acad. Sci. U.S.A. 102*, 2087–2092.
15. Jin, P., Wood, M. D., Wu, Y., Xie, Z. Y., and Katagiri, F. (2003) Cleavage of the *Pseudomonas syringae* type III effector AvrRpt2 requires a host factor(s) common among eukaryotes and is important for AvrRpt2 localization in the host cell. *Plant Physiol. 133*, 1072–1082.
16. Schutkowski, M., Wöllner, S., and Fischer, G. (1995) Inhibition of peptidyl-prolyl *cis*/*trans* isomerase activity by substrate analog structures: Thioxo tetrapeptide-4- nitroanilides. *Biochemistry 34*, 13016–13026.
17. Kern, D., Kern, G., Scherer, G., Fischer, G., and Drakenberg, T. (1995) Kinetic analysis of cyclophilin-catalyzed prolyl *cis*/*trans* isomerization by dynamic NMR spectroscopy. *Biochemistry 34*, 13594–13602.
18. Bosco, D. A., Eisenmesser, E. Z., Pochapsky, S., Sundquist, W. I., and Kern, D. (2002) Catalysis of *cis*/*trans* isomerization in native HIV-1 capsid by human cyclophilin A. *Proc. Natl. Acad. Sci. U.S.A. 99*, 5247–5252.
19. Howard, B. R., Vajdos, F. F., Li, S., Sundquist, W. I., and Hill, C. P. (2003) Structural insights into the catalytic mechanism of cyclophilin A. *Nat. Struct. Biol. 10*, 475–481.
20. Zhao, Y. D., and Ke, H. M. (1996) Mechanistic implication of crystal structures of the cyclophilin dipeptide complexes. *Biochemistry 35*, 7362–7368.
21. Eckert, B., Martin, A., Balbach, J., and Schmid, F. X. (2005) Prolyl isomerization as a molecular timer in phage infection. *Nat. Struct. Mol. Biol. 12*, 619–623.
22. Pletneva, E. V., Sundd, M., Fulton, D. B., and Andreotti, A. H. (2006) Molecular details of Itk activation by prolyl isomerization and phospholigand binding: The NMR structure of the Itk SH2 domain bound to a phosphopeptide. *J. Mol. Biol. 357*, 550–561.
23. Lummis, S. C. R., Beene, D. L., Lee, L. W., Lester, H. A., Broadhurst, R. W., and Dougherty, D. A. (2005) *Cis-trans* isomerization at a proline opens the pore of a neurotransmitter-gated ion channel. *Nature 438*, 248–252.
24. Sarkar, P., Reichman, C., Saleh, T., Birge, R. B., and Kalodimos, C. G. (2007) Proline *cis-trans* isomerization controls autoinhibition of a signaling protein. *Mol. Cell 25*, 413–426.
25. Nelson, C. J., Santos-Rosa, H., and Kouzarides, T. (2006) Proline isomerization of histone H3 regulates lysine methylation and gene expression. *Cell 126*, 905–916.
26. Colgan, J., Asmal, M., Neagu, M., Yu, B., Schneidkraut, J., Lee, Y., Sokolskaja, E., Andreotti, A., and Luban, J. (2004) Cyclophilin A regulates TCR signal strength in CD4(+) T cells via a proline-directed conformational switch in Itk. *Immunity 21*, 189–201.
27. Zhou, X. Z., Kops, O., Werner, A., Lu, P. J., Shen, M. H., Stoller, G., Kullertz, G., Stark, M., Fischer, G., and Lu, K. P. (2000) Pin1-dependent prolyl isomerization regulates dephosphorylation of Cdc25C and tau proteins. *Mol. Cell 6*, 873–883.
28. Fischer, G., and Wawra, S. (2006) Polypeptide binding proteins: What remains to be discovered? *Mol. Microbiol. 61*, 1388–1396.
29. Dugave, C., and Demange, L (2003) *Cis-trans* isomerization of organic molecules and biomolecules: Implications and applications. *Chem. Rev. 103*, 2475–2532.
30. Martin, A., and Schmid, F. X. (2003) A proline switch controls folding and domain interactions in the gene-3-protein of the filamentous phage fd. *J. Mol. Biol. 331*, 1131–1140.
31. Fanghänel, J., and Fischer, G. (2003) Thermodynamic characterization of the interaction of human cyclophilin 18 with cyclosporin A. *Biophys. Chem. 100*, 351–366.
32. Wallace, A. C., Laskowski, R. A., and Thornton, J. M. (1996) Derivation of 3D coordinate templates for searching structural databases: Application to Ser-His-Asp catalytic triads in the serine proteinases and lipases. *Protein Sci. 5*, 1001–1013.
33. Garcia-Echeverria, C., and Rich, D. H. (1995) Kinetic studies of papain: Effect of P3′ substituents and donor/acceptor pairs of intramolecularly quenched fluorogenic substrates. *Lett. Pept. Sci. 2*, 77–82.
34. Scherer, G., Kramer, M. L., Schutkowski, M., Reimer, U., and Fischer, G. (1998) Barriers to rotation of secondary amide peptide bonds. *J. Am. Chem. Soc. 120*, 5568–5574.
35. Brömme, D., Peters, K., Fink, S., and Fittkau, S. (1986) Enzyme-substrate interactions in the hydrolysis of peptide substrates by thermitase, subtilisin BPN′, and proteinase K. *Arch. Biochem. Biophys. 244*, 439–446.
36. Scholz, C., Scherer, G., Mayr, L. M., Schindler, T., Fischer, G., and Schmid, F. X. (1998) Prolyl isomerases do not catalyze isomerization of non-prolyl peptide bonds. *Biol. Chem. 379*, 361–365.
37. Schiene, C., Reimer, U., Schutkowski, M., and Fischer, G. (1998) Mapping the stereospecificity of peptidyl prolyl *cis*/*trans* isomerases. *FEBS Lett. 432*, 202–206.
38. Ingles, D. W., and Knowles, J. R. (1967) Specificity and stereospecificity of α-chymotrypsin. *Biochem. J. 104*, 369–377.
39. Fischer, G. (1994) Peptidyl-prolyl *cis*/*trans* isomerases and their effectors. *Angew. Chem., Int. Ed. 33*, 1415–1436.
40. Quemeneur, E., Moutiez, M., Charbonnier, J. B., and Menez, A. (1998) Engineering cyclophilin into a proline-specific endopeptidase. *Nature 391*, 301–304.
41. Nicastro, G., Menon, R. P., Masino, L., Knowles, P. P., McDonald, N. Q., and Pastore, A. (2005) The solution structure of the Josephin domain of ataxin-3: Structural determinants for molecular recognition. *Proc. Natl. Acad. Sci. U.S.A. 102*, 10493–10498.
42. Wolthers, B. C. (1969) Kinetics of inhibition of papain by TLCK and TPCK in the presence of a BAEE substrate. *FEBS Lett. 2*, 143–145.
43. Wlodawer, A., and Gustchina, A. (2000) Structural and biochemical studies of retroviral proteases. *Biochim. Biophys. Acta 1477*, 16–34.
44. Ellis, V. (2003) in Plasminogen: Structure, activation, regulation (Waisman, D. M., Ed.) pp 26−30, Kluwer Academic/Plenum Publishers, New York.

45. Parry, M. A. A., Zhang, X. C., and Bode, W. (2000) Molecular mechanisms of plasminogen activation: Bacterial cofactors provide clues. *Trends Biochem. Sci. 25*, 53–59.
46. Gros, P., Milder, F. J., and Janssen, B. J. C. (2008) Complement driven by conformational changes. *Nat. Rev. Immunol. 8*, 48–58.
47. Jing, H., Babu, Y. S., Moore, D., Kilpatrick, J. M., Liu, X. Y., Volanakis, J. E., and Narayana, S. V. L. (1998) Structures of native and complexed complement factor D: Implications of the atypical His57 conformation and self-inhibitory loop in the regulation of specific serine protease activity. *J. Mol. Biol. 282*, 1061–1081.